



# CHORUS

This is the accepted manuscript made available via CHORUS. The article has been published as:

## Molecular doping of graphene with ammonium groups

L. Tsetseris and S. T. Pantelides

Phys. Rev. B **85**, 155446 — Published 24 April 2012

DOI: [10.1103/PhysRevB.85.155446](https://doi.org/10.1103/PhysRevB.85.155446)

# Molecular doping of graphene with ammonium groups

L. Tsetseris<sup>1,2</sup> and S. T. Pantelides<sup>2,3,4</sup>

<sup>1</sup>*Department of Physics, National Technical University of Athens, GR-15780 Athens, Greece*

<sup>2</sup>*Department of Physics and Astronomy, Vanderbilt University, Nashville, Tennessee 37235, USA*

<sup>3</sup>*Department of Electrical Engineering and Computer Science,*

*Vanderbilt University, Nashville, Tennessee 37235, USA*

<sup>4</sup>*Oak Ridge National Laboratory, Oak Ridge, Tennessee 37831, USA*

(Dated: March 21, 2012)

Successful doping of an electronic material entails the existence of stable dopant configurations that cause a shift in the Fermi level without altering significantly the electronic states of the host system. The selection of chemical groups that satisfy these conditions when adsorbed on graphene is still an open challenge. Here we show with first-principles calculations that ammonium groups meet the criteria of stable physisorption and efficient doping of graphene. We also describe processes of deactivation of ammonium dopants through their dissociation over graphene impurities or nanoribbon edges. Finally, we show that carbon nanotubes can be used to spatially confine the dopants and avert their edge-related de-activation.

PACS numbers:

## I. INTRODUCTION

Graphene nanoribbons (GNR), stripes of carbon nanosheets with finite width, are being intensely pursued as building blocks in future electronic devices.<sup>1–5</sup> One of the main challenges, in this respect, is the controlled generation of charge carriers within GNRs. In traditional electronic materials, this challenge is answered by introducing dopant impurities at substitutional sites through implantation. A similar strategy is pursued in carbon-based nano-materials like carbon nanotubes or graphene. However, given the fact that substitutional doping may also give rise to unwanted defects or impurities,<sup>6–10</sup> efforts have focused on alternative methods of doping. Perhaps the most appealing recent approach is doping graphene using adsorbed chemical species, instead of substitutional impurities.<sup>3,5,11</sup>

Theoretical calculations<sup>5,11</sup> have suggested that NO<sub>2</sub>, N<sub>2</sub>O<sub>4</sub>, and NO molecules can act as graphene donors. Experiments,<sup>3</sup> on the other hand, have shown that reactions with ammonia lead to effective doping of GNRs with electrons. However, all these dopant candidates have small energies of physisorption on graphene, typically in the order of 0.1 eV or less.<sup>5,11</sup> For this reason, it is doubtful that they can serve as efficient stable dopants of the graphene basal plane. It is assumed, for example, that NH<sub>3</sub> molecules<sup>3</sup> react with GNR edges and some reaction products, as yet unidentified, act then as dopants. If this scenario is true, it will likely pose the new challenge of finding and preparing those edge morphologies that favor the formation of dopant configurations. Clearly, a simpler solution would be to identify other chemical groups that physisorb more strongly on graphene and shift its Fermi energy inside the valence or conduction bands.

In this article we show that ammonium groups (NH<sub>4</sub>) are ideal candidates for the molecular doping of graphene. They have large physisorption energies (more than 1 eV)

and they transform graphene to an *n*-type material. We also show that NH<sub>4</sub> species dissociate readily at GNR edges by giving away one or two H atoms. The deactivation of dopants at GNR edges can be suppressed if carbon nanotubes (CNT) are used to block the migration of NH<sub>4</sub> groups and trap them within areas of the graphene basal plane. In this way, the two indispensable conditions of successful molecular doping, injection of carriers and dopant stability, are satisfied.

## II. METHOD

The results were obtained with the density-functional theory code VASP<sup>12</sup> using ultra-soft pseudopotentials<sup>13</sup> for the valence electrons. We used a local-density approximation (LDA) exchange and correlation (xc) functional<sup>14</sup> and an energy cutoff of 300 eV for the plane-wave basis. For selected configurations we also used a generalized gradient approximation (GGA) xc-functional.<sup>15</sup> It is known that GGA results normally underestimate binding on *sp*<sup>2</sup> carbon, especially for physisorbed configurations.<sup>16–18</sup> Reaction barriers were obtained with the nudged elastic band method,<sup>19</sup> which in previous studies<sup>20,21</sup> provided activation energies in good agreement with experimental data.

The supercells for calculations on a graphene layer contained 160 carbon atoms in a simulation box with in-plane dimensions of 19.65 Å and 21.27 Å. Total energy calculations for this case used the Monkhorst-Pack<sup>24</sup> scheme for sampling of the reciprocal space and a 3×3×1 *k*-mesh. Calculations of electronic densities of states (DOS) employed the tetrahedron method<sup>25</sup> and 9 × 9 × 2 grids for *k*-point sampling. The supercells used in the case of zig-zag GNRs contained 128 carbon atoms and had in-plane dimensions of 19.65 Å and 25.08 Å. The edges of the nano-ribbons were passivated with hydrogen atoms. The actual width of the GNRs was about 17.73

Å. The simulations for the hybrid CNT-graphene system used supercells with in-plane dimensions of 42.53 Å and 14.73 Å, with the latter being the size along the CNT axis. The supercells contained 384 C atoms, 240 of those on the graphene layer and the rest in an arm-chair (6,6) CNT. Total-energy calculations for the zig-zag GNR and CNT-graphene systems used the  $\Gamma$  point for sampling of reciprocal space. The thickness of empty spaces between periodic images in the third out-plane direction was at least 10 Å.

### III. RESULTS AND DISCUSSION

In the following we describe the details of adsorption and the associated electronic effects of ammonia-related groups on pristine and defective graphene. First, we present results for physisorbed  $\text{NH}_3$  and  $\text{NH}_4$  species on a defect-free graphene layer. We then focus on possible de-activation processes for the ammonium dopants either on the graphene basal plane or at GNR edges. We conclude with results on blocking the  $\text{NH}_4$  migration by using CNTs on graphene.

#### A. $\text{NH}_3$ -related species on a pristine graphene layer

The interaction between physisorbed  $\text{NH}_3$  molecules and a pristine graphene layer is weak. According to our calculations, various molecular configurations are possible, but the binding energy for all of the them is less than 0.12 eV. The nitrogen atom of the physisorbed molecule is located 3.1 Å above the graphene layer. The results are in agreement with those already reported in previous studies<sup>11</sup> on the binding energies of physisorbed  $\text{NH}_3$  molecules on graphene. Also in agreement with those studies,<sup>11</sup> we found that physisorbed ammonia molecules do not have a tangible effect on the electronic density of states of graphene close to the Fermi level. Because of these results we can infer that ammonia molecules are not good candidates for effective molecular doping of graphene.

Hydrogen is an ubiquitous impurity in electronic devices,<sup>22,23,26</sup> playing both beneficial and detrimental roles depending on growth and operating conditions. Reactions between physisorbed  $\text{NH}_3$  molecules and hydrogen adatoms generate chemical species that have stronger interactions with the graphene layer. Specifically, an isolated H impurity on graphene can be captured by an  $\text{NH}_3$  molecule in an exothermic reaction that releases 1.00 eV of energy. The  $\text{NH}_4$  group remains close to the graphene layer with its N atom in a distance of 2.7 Å from the carbon sheet. Two of the  $\text{NH}_4$  hydrogen atoms point towards the graphene sheet, while the other two H species are on the other side of the ammonium group. The binding energy against separation of the  $\text{NH}_4$  impurity from the layer is 1.55 eV. This value is large enough to suggest

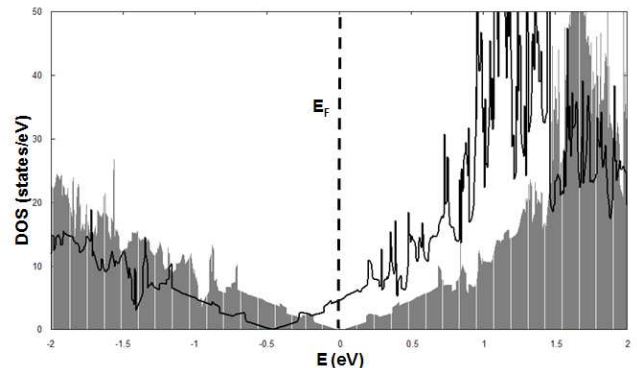


FIG. 1: Electronic density of states (DOS) for graphene with no impurities (shaded area) and with a physisorbed  $\text{NH}_4$  group (black solid line).  $E_F$  is the Fermi level.

that  $\text{NH}_4$  desorption off graphene requires annealing at high temperatures.

The stabilization of ammonium on graphene has a pronounced effect on the electronic properties of the system. The data depicted in Fig. 1 demonstrate that reactions with  $\text{NH}_4$  is an effective means of molecular doping of graphene. The attachment of one ammonium group per 160 carbon atoms gives rise to a shift of the DOS so that the Fermi level of the  $\text{NH}_4$ -laden system lies within the conduction band. In other words,  $\text{NH}_4$  physisorbed impurities act as donors for the basal plane of graphene. Two  $\text{NH}_4$  groups may react to form a hydrogen molecule and two  $\text{NH}_3$  species. This de-activation reaction, however, is not likely because  $\text{NH}_4$  groups repel each other. In particular, bringing two initially remote ammonium impurities to a distance of 10.53 Å and 4.38 Å raises the energy by 0.30 eV and 0.61 eV, respectively. On the other hand, an  $\text{NH}_4$  donor can be de-activated through a reaction with another H impurity of graphene. The process creates  $\text{H}_2$  and  $\text{NH}_3$  molecules and releases 1.42 eV of energy.

The results described above reveal a complex dynamics for ammonia-related species on graphene. One possible scenario to achieve *n*-type doping with ammonium cations is to anneal in an  $\text{NH}_3$  ambient a graphene sample with a small number of atomic H impurities. In this way, a number of  $\text{NH}_4$  donors can be formed by the direct reaction of the H adatoms with the ammonia molecules. If the temperature is subsequently raised, then the weakly physisorbed  $\text{NH}_3$  molecules will desorb off graphene, leaving behind strongly physisorbed ammonium dopants.

#### B. De-activation of $\text{NH}_4$ dopants on graphene

Though ammonium donors are stable against dissociation when they are over a pristine graphene layer, they may dissociate when they arrive close to graphene defects or impurities. One example relates to the breakup of the  $\text{NH}_4$  group in the vicinity of a substitutional N impurity.

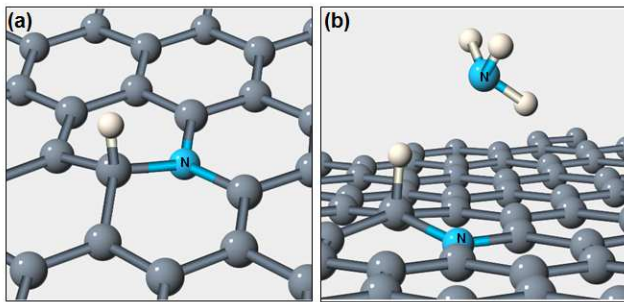


FIG. 2: (Color online) (a) N-H complex: H atom trapped at a substitutional N dopant site of graphene. (b) a NH<sub>3</sub> molecule physisorbed over a N-H complex. [C: gray, N: light gray (cyan), H: white spheres]

As shown in Fig. 2(b), the ammonium cation deposits one of its H atoms to a C site next to the N impurity, forming thus an N-H complex on graphene. The energy gain of this process is about 0.10 eV. The N atom of the NH<sub>3</sub> molecule is attracted by the H atom of the N-H complex and the interaction results in a sizeable binding energy of 0.27 eV. A finite value of 0.12 eV is obtained also using GGA calculations. Annealing in elevated temperatures may force the NH<sub>3</sub> molecule to desorb. The N-H complex, on the other hand, is more resilient because it has a significant binding energy of 0.55 eV against release of its H atom to a remote graphene position.

The formation of the N-H complex modifies the DOS of graphene as shown in the related data of Fig. 3. While pristine graphene has a vanishing band gap at the Fermi level ( $E_F$ ), one N-H complex per 160 graphene sites creates a peak right below  $E_F$  and induces a small gap of 0.18 eV. This effect constitutes a significant deviation from the ideal doping profile of an isolated substitutional N impurity. The DOS associated with the N-H complex differ significantly also from the DOS profile on an isolated H impurity on graphene. H-related DOS data show that the impurity generates a band gap of 0.5 eV and a narrow, strong peak in the middle of the gap. On the other hand, the effect of the stable N-H-NH<sub>3</sub> complex of Fig. 2(b) on the DOS of graphene resembles that of the N-H defect. The corresponding DOS data of Fig. 3 show that physisorption of the NH<sub>3</sub> molecule narrows slightly the N-H related DOS peak and opens an additional small gap between this peak and the rest of the valence band.

### C. De-activation of NH<sub>4</sub> dopants at graphene edges

The dissociation of NH<sub>4</sub> species at N substitutional sites is an adverse effect with respect to graphene doping. However, the importance of this dissociation scenario is limited only to those graphene samples that have significant numbers of N substitutional impurities. In contrast, the de-activation pathway we will discuss in the following poses a more prevalent risk to the NH<sub>4</sub>-induced doping

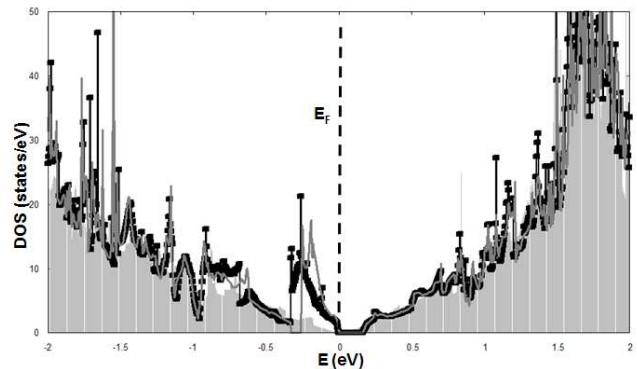


FIG. 3: Electronic density of states (DOS) for graphene with no impurities (shaded area), with one N-H complex of the type shown in Fig. 2(a) (black line with squares), and with the complex of Fig. 2(b) (gray line).  $E_F$  is the Fermi level.

scheme because it relates to reactions at the ever present edges of a graphene layer. In particular, we have found that an NH<sub>4</sub> dopant dissociates readily when it arrives at the zig-zag edge of a graphene nano-ribbon. At first, an NH<sub>4</sub> group that is brought above an edge C atom of a GNR transforms spontaneously (in a barrier-less process) to an NH<sub>3</sub> molecule by releasing one of its H atoms to an edge ethylene (CH<sub>2</sub>) group. A second breakup reaction may then ensue. Following a multi-step dissociation process, the ammonia molecule may release a H atom to a neighboring edge C atom, while the NH<sub>2</sub> amine moiety gets attached to another C edge site. The configuration is shown in Fig. 4(b). Its energy is 0.1 eV lower than that of the NH<sub>3</sub> structure of Fig. 4(a). The breakup of the NH<sub>3</sub> molecule has a barrier of 0.6 eV.

The system is stabilized further when the H atom hops away from the NH<sub>2</sub> group to another C edge atom. Specifically, the configuration depicted in Fig. 4(c) is more stable than the geometry of Fig. 4(a) by 0.65 eV. The corresponding GGA energy difference is 0.08 eV. Another 0.2 eV is gained when the released H atom migrates to more remote sites. The results on the energies of the above structures are summarized in Table 4. Other possible structures include C-NH<sub>2</sub> groups as protrusions at the edge and a released H<sub>2</sub> molecule, or a C-NH<sub>3</sub> edge group and a released H atom on a neighboring edge C atom. These types of geometries have, in fact, been employed in previous studies<sup>27-29</sup> on N-related doping of graphene nano-ribbons. Compared to the most stable structure of the type of Fig. 4(c), however, the C-NH<sub>2</sub> and C-NH<sub>3</sub> edge configurations lie higher in energy by more than 1 eV.

### D. NH<sub>4</sub> trapping by carbon nanotubes on graphene

As mentioned above, the dissociation of NH<sub>4</sub> species at GNR edges poses the challenge of how to retain a non-negligible number of ammonium dopants over graphene.

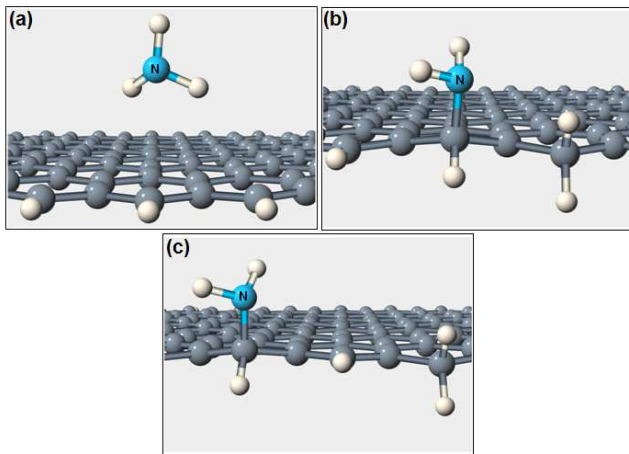


FIG. 4: (Color online) Adsorption of a  $\text{NH}_3$  molecule at the edge of zig-zag graphene nano-ribbon: (a) physisorbed  $\text{NH}_3$ , (b) and (c) chemisorbed  $\text{NH}_2$  group and a H atom following the dissociation of the  $\text{NH}_2$  molecule. [C: gray, N: light gray (cyan), H: white spheres]

TABLE I: Relative stability of  $\text{NH}_3$ -related configurations at the edge of a zig-zag graphene nanoribbon. The energy of the most stable structure is set to zero.

Figure	Description	E (eV)
Fig. 4(a)	Physisorbed $\text{NH}_3$	0.85
Fig. 4(b)	Proximal $\text{NH}_2$ and $\text{CH}_2$ units	0.75
Fig. 4(c)	Remote $\text{NH}_2$ and $\text{CH}_2$ units	0.20
	Isolated $\text{NH}_2$ and $\text{CH}_2$ units	0.00

We have found that there is a very small spread of energies, less than 0.1 eV, for neighboring  $\text{NH}_4$  configurations over graphene. This tiny energy difference suggests that the diffusion barrier is also very small and that the  $\text{NH}_4$  dopants migrate rapidly over graphene. Therefore, the ammonium-based doping scheme can be successful only under conditions that block the movement of the physisorbed species towards the GNR edge. In the following we show that this role can be played by carbon nanotubes that are deposited on graphene.

Figure 5 depicts a number of configurations for

TABLE II: Relative stability of the  $\text{NH}_4$ -related configurations shown in Fig. 5. The second column describes the relative position of the  $\text{NH}_4$ -related species with respect to the carbon nanotube (CNT) and the graphene layer (GL). The energy of the most stable structure is set to zero.

Figure	Description	E (eV)
Fig. 5(a)	wedged between CNT and GL	0.00
Fig. 5(b)	on the GL, away from the CNT	0.50
Fig. 5(c)	on top of the CNT	0.90
Fig. 5(d)	H adatom- $\text{NH}_3$ complex on the CNT	0.90

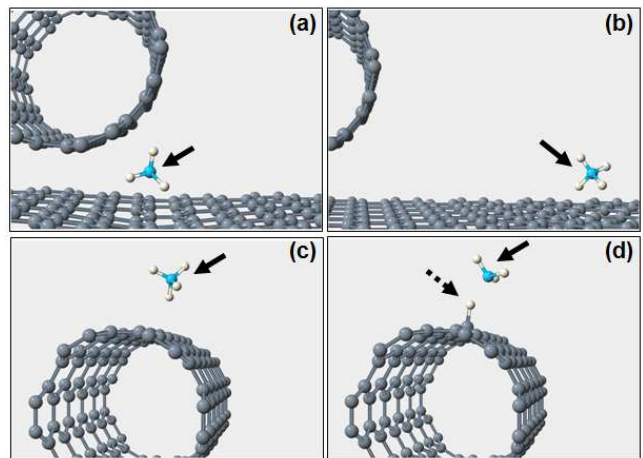


FIG. 5: (Color online) Configurations for  $\text{NH}_4$  related species in a hybrid graphene-carbon nanotube (CNT) system: (a)  $\text{NH}_4$  wedged between graphene and a (6,6) CNT, (b)  $\text{NH}_4$  over graphene, (c)  $\text{NH}_4$  physisorbed only on the CNT, and (d) complex between a H adatom (shown with a dotted arrow) on the CNT and an  $\text{NH}_3$  molecule (shown with a solid arrow). The arrows in (a)-(c) point to the  $\text{NH}_4$  group. [C: gray, N: light gray (cyan), H: white spheres]

ammonium-related species in a system that comprises graphene and a (6,6) CNT. In the most stable geometry of Fig. 5(a) the  $\text{NH}_4$  cation is wedged between the CNT and the graphene layer. The energy of the configuration of Fig. 5(b), wherein the  $\text{NH}_4$  is physisorbed on graphene, but away from the CNT, is 0.5 eV higher. When the  $\text{NH}_4$  is lifted away from graphene, but remains close to the CNT, the energy increases by 0.9 eV. An energy increase of about 0.9 eV accompanies also the dissociation of ammonium over the CNT and formation of a complex between a chemisorbed H atom and a physisorbed  $\text{NH}_3$  molecule. The last two structures are shown in Figs. 5(c)-(d). The results on the relative stability of the above structures are summarized in Table II

These results show that it is energetically favorable for a  $\text{NH}_4$  group to stay on one side of the CNT, and not climb over the nanotube either as physisorbed, or as chemisorbed species. This fact effectively means that CNTs can be used as walls to trap the  $\text{NH}_4$  (or, possibly, other molecules of choice) within certain areas over graphene. There is an energetic preference for the  $\text{NH}_4$  cation to physisorb close to the CNT, but the relatively small energy difference of 0.5 eV, combined with the fact that  $\text{NH}_4$  groups repel each other, suggest that a significant number of ammonium dopants can be stabilized on the graphene basal plane. In addition, future studies can explore variants that could decrease the effect of dopant wedging between the graphene sheet and a CNT fence, averting thus the scenario of inhomogeneous distribution of dopants. For example,  $\text{NH}_4$  wedging could be partly frustrated in the case of CNTs that have been functionalized with electropositive chemical units.

## IV. SUMMARY

Using first-principles calculations we have identified ammonium groups as graphene donors. Unlike other small molecular species, the  $\text{NH}_4$  radicals have a large binding energy of 1.3 eV when they are physisorbed on graphene. Carbon nanotubes can trap these dopants over certain areas of a graphene layer, suppressing their de-activation through dissociation reactions at graphene nano-ribbon edges.

## V. ACKNOWLEDGEMENTS

The work was supported by the McMinn Endowment at Vanderbilt University, by the US Department of Energy Basic Energy Sciences, and by Grant No HDTRA 1-10-10016. The calculations were performed at ORNL's Center for Computational Sciences.

- 
- <sup>1</sup> T. Lohmann, K. von Klitzing, and J. H. Smet, *Nano Lett.* **9**, 1973 (2009).
- <sup>2</sup> J. D. Fowler, M. J. Allen, V. C. Tung, Y. Yang, R. B. Kaner, and B. H. Weiller, *ACS Nano* **3**, 301 (2009).
- <sup>3</sup> X. Wang, X. Li, L. Zhang, Y. Yoon, P. K. Weber, H. Wang, J. Guo, and H. Da, *Science* **324**, 768 (2009).
- <sup>4</sup> F. Schwierz, *Nature Nanotechn.* **5**, 487 (2010).
- <sup>5</sup> T. O. Wehling, K. S. Novoselov, S. V. Morozov, E. E. Vdovin, M. I. Katsnelson, A. K. Geim, and A. I. Lichtenstein, *Nano Lett.* **8**, 173 (2008).
- <sup>6</sup> D. S. L. Abergel, V. Apalkov, J. Berashevich, K. Ziegler, T. Chakraborty, *Adv. Phys.* **59**, 261 (2010).
- <sup>7</sup> B. Wang and S. T. Pantelides, *Phys. Rev. B* **83**, 245403 (2011).
- <sup>8</sup> D. Wei, Y. Liu, Y. Wang, H. Zhang, L. Huang, and G. Yu, *Nano Lett.* **9**, 1752 (2009).
- <sup>9</sup> B. Guo, Q. Liu, E. Chen, H. Zhu, L. Fang, and J. R. Gong, *Nano Lett.* **10**, 4975 (2010).
- <sup>10</sup> Y. C. Lin, C. Y. Lin, and P. W. Chiu, *Appl. Phys. Lett.* **96**, 133110 (2010).
- <sup>11</sup> O. Leenearns, B. Partoens, and F. M. Peeters, *Phys. Rev. B* **77**, 125416 (2008).
- <sup>12</sup> G. Kresse and J. Furthmuller, *Phys. Rev. B* **54**, 11 169 (1996).
- <sup>13</sup> D. Vanderbilt, *Phys. Rev. B* **41**, 7892 (1990).
- <sup>14</sup> J. P. Perdew and A. Zunger, *Phys. Rev. B* **23**, 5048 (1981).
- <sup>15</sup> J. P. Perdew and Y. Wang, *Phys. Rev. B* **45**, 13244 (1992).
- <sup>16</sup> L. Tsetseris and S. T. Pantelides, *Appl. Phys. Lett.* **87**, 233109 (2005); L. Tsetseris and S. T. Pantelides, *Phys. Rev. B* **75**, 153202 (2007).
- <sup>17</sup> L. Tsetseris and S. T. Pantelides, *Phys. Rev. Lett.* **97**, 266805 (2006); L. Tsetseris and S. T. Pantelides, *Phys. Rev. B* **82**, 045201 (2010).
- <sup>18</sup> L. A. Girifalco and M. Hodak, *Phys. Rev. B* **65**, 125404 (2002).
- <sup>19</sup> G. Mills, H. Jónsson, and G. K. Schenter, *Surf. Sci.* **324**, 305 (1995).
- <sup>20</sup> L. Tsetseris, X. J. Zhou, D. M. Fleetwood, R. D. Schrimpf, and S. T. Pantelides, *IEEE Trans. Device Mater. Reliab.* **7**, 502 (2007).
- <sup>21</sup> L. Tsetseris, N. Kalfagiannis, S. Logothetidis, and S. T. Pantelides, *Phys. Rev. B* **76**, 224107 (2007).
- <sup>22</sup> S. T. Pantelides, L. Tsetseris, S. N. Rashkeev, X. J. Zhou, D. M. Fleetwood, and R. D. Shrimpf, *Microelectron. Reliab.* **47**, 903 (2007).
- <sup>23</sup> L. Tsetseris, D. M. Fleetwood, R. D. Schrimpf, X. J. Zhou, I. G. Batyrev, and S. T. Pantelides, *Microelectron. Eng.* **84**, 2344 (2007).
- <sup>24</sup> D. J. Chadi, and M. L. Cohen, *Phys. Rev. B* **8**, 5747 (1973).
- <sup>25</sup> O. Jepson and O. K. Andersen, *Solid State Commun.* **9**, 1763 (1971).
- <sup>26</sup> L. Tsetseris and S. T. Pantelides, *J. Phys. Chem. B* **113**, 941 (2009).
- <sup>27</sup> F. Cervantes-Sodi, G. Csnyi, S. Piscanec, and A. C. Ferrari, *Phys. Rev. B* **77**, 165427 (2008).
- <sup>28</sup> H. Lee, *J. Phys. Condens. Matter* **22**, 352205 (2010).
- <sup>29</sup> A. P. Seitsonen, A. M. Saitta, T. Wassmann, M. Lazzeri, and F. Mauri, *Phys. Rev. B* **82**, 115425 (2010).